An FPGA-based, multi-channel, real-time, motion artifact detection technique for fNIRS/DOT systems

Yunjia Xia
HUB of Intelligent Neuro-engineering (HUBIN), DSIS
University College London(UCL)
London, UK
yunjia.xia.18@ucl.ac.uk

Elisabetta Maria Frijia
DOT-HUB, Department of Medical Physics and Biomedical Engineering
University College London(UCL)
London, UK
elisabetta.frijia.18@ucl.ac.uk

Rui Loureiro
Division of Surgery & Interventional Science(DSIS)
University College London(UCL)
London, UK
r.loureiro@ucl.ac.uk

Robert J. Cooper
DOT-HUB, Department of Medical Physics and Biomedical Engineering
University College London(UCL)
London, UK
robert.cooper@ucl.ac.uk

Hubin Zhao
HUB of Intelligent Neuro-engineering (HUBIN), DSIS
University College London(UCL)
London, UK
hubin.zhao@ucl.ac.uk

***Abstract*— Functional Near-Infrared Spectroscopy (fNIRS) and its extension, Diffuse Optical Tomography (DOT), are emerging non-invasive neuroimaging techniques that measure brain activities by monitoring changes in blood oxygenation using near infrared light. However, motion artifacts from subject movements in fNIRS/DOT data could severely undermine data quality. Current solutions typically rely on offline methods executed on conventional computers in laboratories/hospitals, limiting real-time applications and flexibility in wider environments. To address these limitations, we present an FPGA-based multi-channel real-time motion artifact detection system. The proposed system, tested against an expert-annotated dataset, showcases encouraging overall performance, with a minimal delay of 2.75 ms across 12-channel raw fNIRS data, and boasts a sensitivity rate of 85.28% and accuracy of 87.06%. This efficiency is achieved using less than 10% of FPGA resources, underscoring that the proposed real-time processing system holds the potential to be scaled up to 3630 channels. These results indicate a promising avenue towards real-time motion artifact processing in large-size multi-channel fNIRS/DOT data. Our design lays the groundwork for its application in areas including wearable real-time functional brain imaging, brain-computer interfaces, human-robot interaction, and surgical monitoring.**

Keywords*— *functional near-infrared spectroscopy, diffuse optical tomography, motion artifact, real-time, FPGA, wearable.

I. Introduction

Functional Near-Infrared Spectroscopy (fNIRS) is a non-invasive, portable neuroimaging technique [1],[2]. It capitalizes on the unique absorption spectra of oxygenated and deoxygenated forms of hemoglobin, the molecule responsible for oxygen transport in the bloodstream, within the near-infrared wavelength range (Fig. 1a). As depicted in Fig. 1b, a near-infrared light source and a detector are positioned on the scalp. This setup, consisting of the light source and the detector, is referred to as an optical channel. By observing variations in the intensity of near-infrared light as it traverses the scalp and brain (as shown in Fig. 1b), it is possible to deduce changes in the concentration of oxy-hemoglobin (HbO) and deoxy-hemoglobin (HbR). Due to the distinct absorption characteristics of HbO and HbR within the near-infrared spectrum, analyzing these differential absorption rates across specific wavelengths allows for the determination of changes in their concentrations. Such concentration

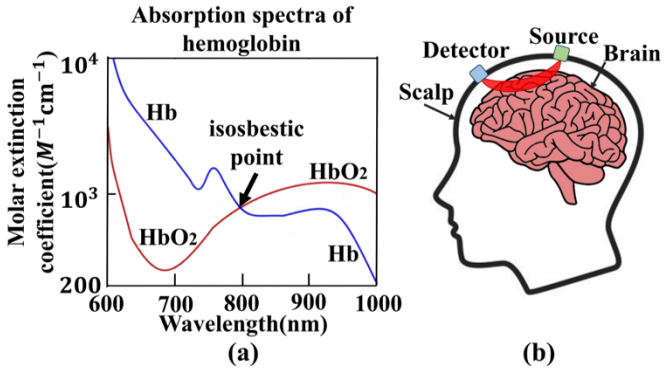

Fig. 1 a) The absorption spectra of HbO and HbR in the Near-Infrared Wavelength Range (650 to ~1000 nm). fNIRS systems typically operate at two wavelengths, usually with one above and one below the isosbestic point (808nm), at which HbO and HbR demonstrate the same absorption coefficient; b) Illustration of the source-detector pair in an fNIRS system, depicting the light path.

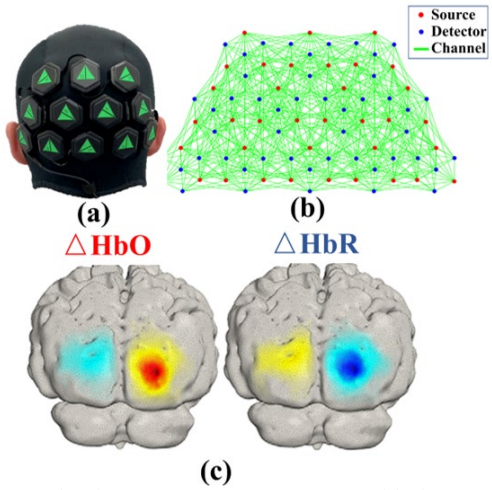

Fig. 2 a) Example of a HD-DOT system, LUMO and b) its source-detector array layout; c) Activation maps obtained from visual stimulus using the LUMO HD-DOT system [5].

This research is supported by The Royal Society Research Grant (RGS/R2/222333), Engineering and Physical Sciences Research Council Grant (13171178 R00287), European Research Council (ERC) under the European Union's Horizon Europe Research and Innovation Program (No. 101099093), and Department of Orthopaedics and Musculoskeletal Science/the Wellcome Trust/EPSRC through the WEISS Centre of UCL(203145Z/16/Z).

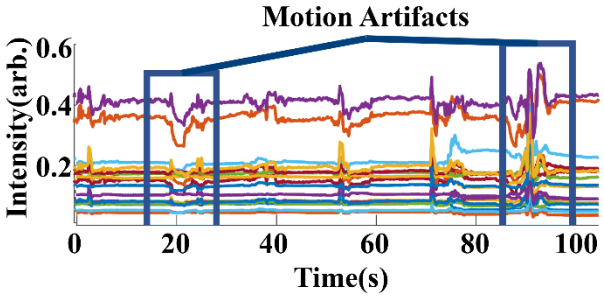

Fig. 3 An example of motion artifacts in fNIRS channel signal.

variations provide valuable insights into cerebral hemodynamic activity.

Diffuse Optical Tomography (DOT) is a more advanced offshoot of fNIRS. By deploying an array of multiple near-infrared light sources and detectors positioned on the scalp, the light emitted from a single source can be detected by several detectors (with various source-detector separations), achieving overlapping spatial sampling for 3D neuroimaging [3]. Building upon this, high-density DOT (HD-DOT) further refines the DOT technique by incorporating a denser, high-density source-detector array. An example of wearable HD-DOT device, LUMO (Gowerlabs Ltd. UK) [4], is shown in Fig. 2a. Sources and detectors are placed beneath the hexagon modules, connected to fibers that directly coupled to the scalp. With a high-density source-detector layout detailed in Fig. 2b, the shown setting of LUMO can provide up to 1728 optical measurement channels[5]. This advanced configuration facilitates improved spatial resolution, empowering the device to generate high-resolution 3D brain activation map shown in Fig. 2c. Furthermore, the incorporation of varied source-detector separation optimizes both lateral and depth specificity. fNIRS, DOT, and HD-DOT have facilitated functional neuroimaging of the human cortex, offering more accessible, portable/wearable, cost-efficient, and user - friendly solutions in diverse settings [6]. Such advancements have the potential to bridge gaps in clinical and healthcare applications, particularly in areas previously constrained by the availability of sophisticated neuroimaging technology, as demonstrated in recent studies [7]–[9].

Despite significant advancements in fNIRS/DOT technologies, subject movements during data collection can impact the collected data quality, as head motions lead to decoupling between the source/detector fiber and the scalp, resulting in high-frequency spikes and shifts from the baseline intensity in the measured signals [10], as illustrated in Fig. 3. For an accurate estimation of the hemodynamic response function (HRF), it is crucial to detect and remove these motion artifacts. While numerous methods for motion artifact detection and correction have been proposed, the majority operate offline after the experiment has concluded [10]. Such post-experiment processing, compared to real-time (online) detection, is less efficient, risking missed data and not adjusting promptly to a subject's in-session behavior. These limitations increasingly underscore the importance and demand of advancing real-time processing in fNIRS technology.

Recent studies have introduced various online techniques for fNIRS motion artifact detection. Barker et al. [11] used a modified linear Kalman filter to detect and correct the motion artifact in real-time. Zhao et al. [12] used Targeted median filter for online motion artifact detection. Gao et al. [13] used a convolution neural network based denoising autoencoder (DAE) with the potential to be applied in real-time.

However, these processing techniques are reliant on separated benchtop computers, constraining fNIRS/DOT to laboratory environments and posing challenges related to scalability and increased processing time as the number of measurement channels increases, which is directly related to fNIRS/DOT spatial resolution. Additionally, although these methods might show efficiency for basic fNIRS devices with limited number of channels, systems like DOT and HD-DOT, which have a significantly higher channel number, pose a greater challenge. As the channel number increases, the computational cost and system delay swell due to the augmented processing load and memory requirements for handling a larger dataset. This could potentially affect the efficiency of real-time processing capabilities.

Herein, we proposed an FPGA-based module tailored for real-time, multichannel motion artifact detection in fNIRS/DOT, and the conceptual diagram is illustrated in Fig. 4. The advantages of this design include: (1) The inherent real-

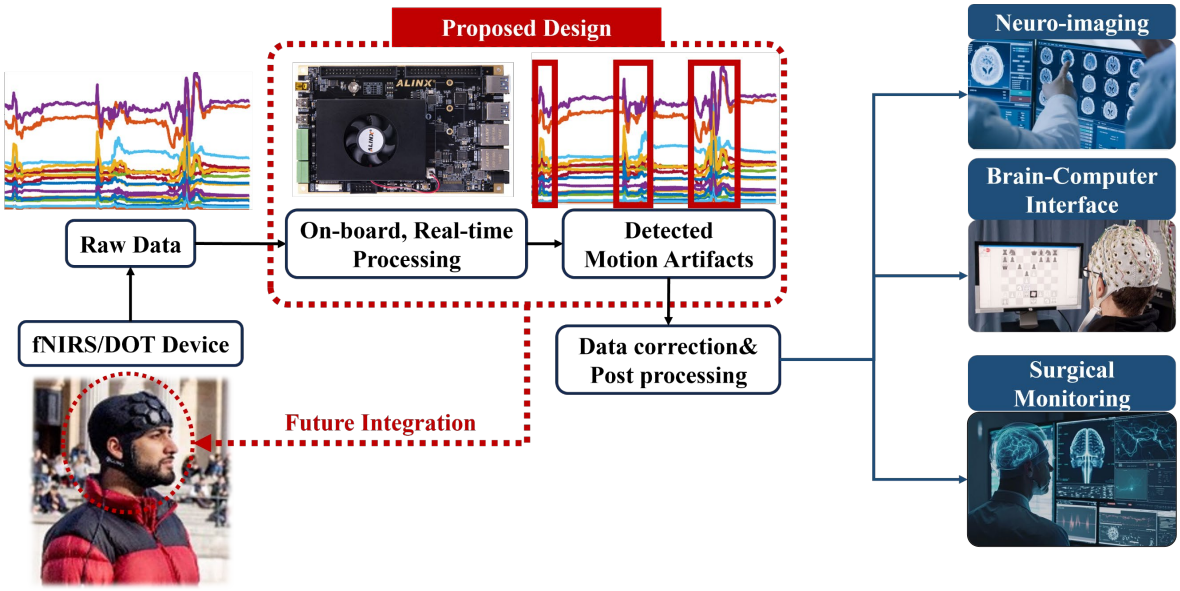

Fig. 4 Overview of the proposed system. The circled area is our proposed design to achieve wearable, real-time motion artifact detection.

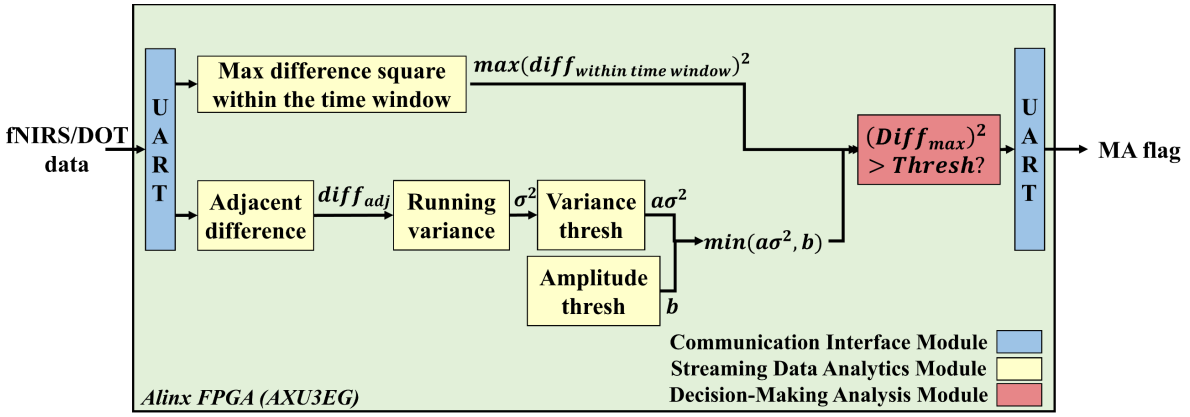

Fig. 5 The architecture of the proposed online motion artifact detection design.

Initialization: $m = S = n = 0$;

for each incoming sample x:

$$mean_{prev} = m;$$

$$n = n + 1;$$

$$m = m + \frac{x - m}{n};$$

$$S = S + (x - m) * (x - mean_{prev});$$

$$Variance = \frac{S}{n}$$

Fig. 6 The online variance calculation in the proposed design.

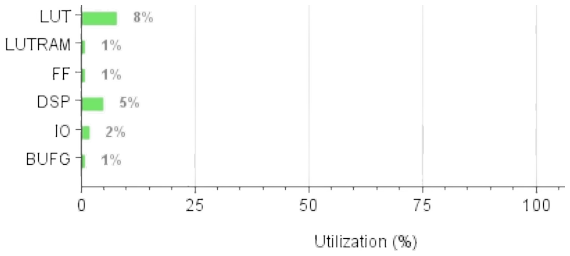

Fig. 7 Visual depiction of the key FPGA resource of proposed design and the utilization of these resources within the FPGA.

time processing proficiency enables instantaneous identification of motion artifacts, ensuring that data quality is maintained throughout the course of fNIRS/DOT monitoring. This immediacy is crucial for applications requiring live feedback, such as neurofeedback training or brain-computer interfaces; (2) Its capability to potentially integrate into current fNIRS/DOT devices, thereby obviating the requirement of a separate computer for motion artifact detection during experiments, and (3) scalability for parallel processing across multiple channels, ensuring fast processing without added delay, which is also suitable for DOT and HD-DOT. This paper is organized as follows: Section II details the proposed motion artifact detection technique; Section III presents and analyzes the experimental results; and Section IV concludes the paper.

II. Proposed Technique

Our approach employs a motion artifact detection method for fNIRS/DOT data that leverages spline interpolation, as advocated by [14]-[15]. This method rests on two premises: (1) The recorded fNIRS signal represents a linear combination of motion artifacts and the uncontaminated fNIRS signal, and (2) within segments corrupted by motion, the artifact component predominantly influences the recorded fNIRS signal. For a streamlined analysis, we identify motion artifacts by assessing both the variance and amplitude changes in adjacent data differences. When the peak squared difference within a specified time window surpasses either the predetermined variance-based threshold or amplitude square thresholds, the relevant data, along with the subsequent data within the time window are marked as motion artifacts.

The overall architecture of our system is presented in Fig. 5. For the fNIRS/DOT data transmission, we employed a Universal Asynchronous Receiver-Transmitter (UART) interface, operating at a baud rate of 115200, to manage data exchange with the corresponding fNIRS/DOT device. The fNIRS/DOT data, which included the received light intensity with five decimal places, was transmitted in hexadecimal format. This interface was responsible for receiving the data and dispatching the flag of motion artifact. The received fNIRS/DOT data was first processed using a simple subtraction logic in the adjacent difference module crafted in Verilog. This processed data was subsequently channeled to the running variance module. Variance computations were conducted using Welford's online algorithm [16]. The computation details are shown in Fig. 6, where x is incoming data sample, m is the current data average and n is the number of the receiver data samples. This logic for variance computation was encoded in Verilog. The computed variance was then multiplied by the variance threshold, achieved using a data shift method, and subsequently compared to the amplitude squared threshold. The minimum threshold was applied to evaluate against the maximal squared difference observed in the fNIRS/DOT data over a designated time window. The parameter pairing for the variance and squared amplitude threshold was ascertained to be 16 and 0.16, respectively. This configuration can effectively distinguish significant data fluctuations attributable to subject movements from the more subtle variations induced by physiological phenomena such as heartbeat. Such discernment is crucial for ensuring that the system robustly detects motion-induced artifacts without erroneously classifying these physiological signals as artifacts.

Concurrently, the fNIRS/DOT data was channeled to the submodule (shown in Fig. 5) computing the maximum squared difference within a specific time window. In this module, the present data is subtracted from the subsequent 11 data points. By comparing these subtraction results pairwise, the maximal difference is ascertained and then squared to align with the same unit as the threshold calculated above. If the squared maximum difference surpasses the threshold, both the data from the current time frame and the following 11 data

points are identified as motion artifacts. The detection result was then transmitted to the UART interface back to the fNIRS/DOT device.

We implemented our design using Verilog and deployed it on a Xilinx AXU3EG FPGA board [17] for performance evaluation. The overall FPGA resource utilization is illustrated in Fig. 7.

To evaluate the system performance of the proposed real-time motion artifact detector, we utilized a HD-DOT dataset collected from infant subjects using a 12-tile LUMO device (Gowerlabs Ltd., UK), which captures fNIRS/DOT data at a sampling rate of 12 Hz. The targeted population, infants, are particularly challenging in the context of fNIRS/DOT data acquisition due to their unpredictable movements, which pose a high risk of introducing motion artifacts into the data.

Each tile of the LUMO system is intricately equipped with three light sources and four detectors. This configuration results in twelve source-detector channels per tile, enabling dense spatial sampling critical for the detailed mapping of cerebral hemodynamics. The compiled dataset is comprised of recordings from ten subjects, each providing data from twelve tiles, which culminates in a total of 144 within-tile channels. The range of the data across subjects is notably diverse, with the shortest span of recording consisting of approximately 1951 data points (~162 seconds) and the longest recording comprising up to 5617 data points (~468 seconds). In total, the dataset amasses more than 32,200 temporal data points, with each timepoint reflecting information from 144 channels of DOT data.

The ground truth result of motion artifact identification within this extensive dataset was collectively conducted by four professionally-trained fNIRS/DOT experts. Given the extensive scale of the dataset and the highly correlated nature of the short channels within each tile, a tile-centric approach was deliberately adopted to mitigate the laboriousness of channel-specific labeling. If any single channel within a tile was observed to contain motion artifacts, the entire tile was marked accordingly. This labeling strategy provided a well-founded basis for the motion artifact detection system, assuring a trustworthy assessment of motion artifacts. The detection outcomes from the FPGA were compared with the expert-labelled ground truth labelled results and depicted in Section III below.

III. Results

The system proposed here delivers rapid decision-making capabilities, evidenced by a minimal delay of 2.75 ms in detecting motion artifacts across 12-channel raw fNIRS/DOT data. The efficient processing of the system at a 12Hz frame rate, using under only 10% of FPGA resources, suggests it could potentially extend to real-time processing of approximately 3630 channels. Fig. 8 visually represents this process, with areas indicating detected motion artifacts distinctly shaded for clarity. Subsequent comparative analysis with manually expert-labeled ground truth data is depicted in Fig. 9.

In evaluating the efficacy of our fNIRS/DOT motion artifact detection system, we computed key performance metrics including sensitivity, specificity, precision, and accuracy. Sensitivity, or the true positive rate (in our case, *positive* means the data has motion artifact), is crucial in this context as it reflects the system's capability to correctly identify instances of motion artifacts, thereby allowing for immediate corrective action during experimental conditions. Specificity measures the system's capacity to correctly discern non-artifact periods, avoiding false alarms that could lead to unnecessary data exclusion or interruptions in data collection. Precision, the proportion of true positives among all positive identifications, underscores the system's exactness, minimizing the risk of discarding valuable data. Lastly, accuracy represents the overall correctness of the system across all classifications, ensuring the system's reliability.

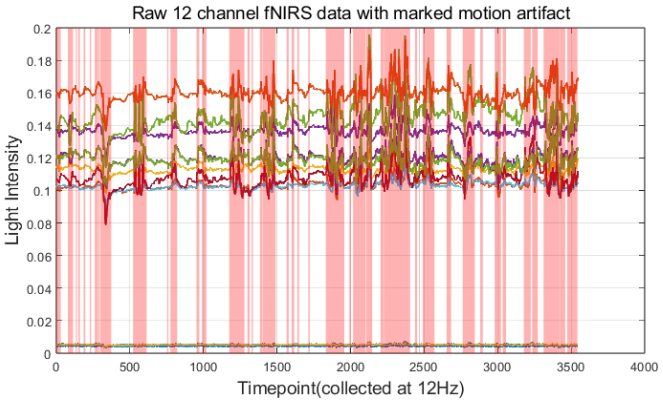

Fig. 8 Raw fNIRS data across 12 channels with shaded regions indicating motion artifacts detected by the proposed design.

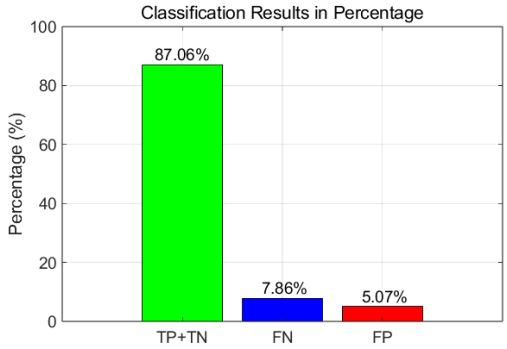

Fig. 9 Detection outcomes as percentages: True Positives (TP)+True Negative (TN), False Negatives (FN), and False Positives (FP).

TABLE I. Performance Metrics of the Proposed Motion Artifact Detection System.

Performance Metric (%)	Proposed System	Homer3 (Traditional)
Sensitivity	85.28	74.94
Specificity	89.11	90.89
Precision	89.98	88.40
Accuracy	87.06	83.21

Our system's performance was rigorously evaluated by comparing its performance against Homer3 [18], a widely adopted MATLAB toolbox for *offline* fNIRS/DOT data analysis and motion artifact detection. The comparison revealed that our system achieved a sensitivity rate of 85.28%, higher than Homer3's 74.94%. Additionally, our accuracy stands at 87.06%, which is an improvement over Homer3's accuracy of 83.21%. These results not only underscore the robustness and reliability of our detection algorithm but also mark a significant step forward in the precision of multi-channel real-time motion artifact detection within this field. Comprehensive performance metrics of the proposed detection system against Homer3 are cataloged in Table I.

IV. Discussion and Conclusion

Our motion artifact detection system showcases an encouraging capability in real-time processing of multi-channel fNIRS/DOT data, achieving a fine sensitivity of 85.28% and an accuracy of 87.06%. These results indicate a high degree of reliability in identifying true motion artifacts, a vital factor in the practical applications of fNIRS/DOT technologies. While benchtop computers might reach comparable processing speeds, our FPGA design stands out due to its inherent advantages. The strong parallel computation capability of FPGA not only ensures clearly faster data processing compared to traditional benchtop computers but also significantly enhances the precision of data acquisition, particularly when managing the vast volumes of data channels associated with DOT/HD-DOT devices.

This real-time processing capability is crucial for the integrity and reliability of emerging fNIRS/DOT-based real-time applications, such as real-time brain imaging, brain-computer interface, human-robot interaction, surgical monitoring, and beyond. Moreover, the portability and cost-effectiveness of FPGA make it suitable for dynamic application environments, negating the necessity for cumbersome and pricey computing infrastructure. For high-channel number DOT devices, the attributes of the FPGA offer a blueprint for smooth integration, bolstering the adaptability and scalability of the devices.

As fNIRS/DOT technologies continue to advance, our FPGA-based multichannel, real-time processing approach marks a pivotal progression, as evidenced by its superior sensitivity and precision in detecting motion artifacts. This innovation fosters a more robust application of fNIRS/DOT methodologies beyond controlled laboratory/hospital settings, ensuring the acquisition of reliable and accurate data even at almost any environment.

References

[1] M. Ferrari and V. Quaresima, "A brief review on the history of human functional near-infrared spectroscopy (fNIRS) development and fields of application," *Neuroimage*, vol. 63, no. 2, pp. 921–935, Nov. 2012, doi: 10.1016/j.neuroimage.2012.03.049.

[2] F. Scholkmann *et al.*, "A review on continuous wave functional near-infrared spectroscopy and imaging instrumentation and methodology," *Neuroimage*, vol. 85, pp. 6–27, Jan. 2014, doi: 10.1016/j.neuroimage.2013.05.004.

[3] H. Zhao and R. J. Cooper, "Review of recent progress toward a fiberless, whole-scalp diffuse optical tomography system," *Neurophotonics*, vol. 5, no. 01, p. 1, Sep. 2017, doi: 10.1117/1.NPh.5.1.011012.

[4] "LUMO — Gowerlabs." Accessed: Oct. 21, 2023. [Online]. Available: https://www.gowerlabs.co.uk/lumo

[5] E. E. Vidal-Rosas *et al.*, "Evaluating a new generation of wearable high-density diffuse optical tomography technology via retinotopic mapping of the adult visual cortex," *Neurophotonics*, vol. 8, no. 2, pp. 1 – 24, 2021, doi: 10.1117/1.NPh.8.2.025002.

[6] E. E. Vidal-Rosas, A. von Lühmann, P. Pinti, and R. J. Cooper, "Wearable, high-density fNIRS and diffuse optical tomography technologies: a perspective," *Neurophotonics*, vol. 10, no. 02, May 2023, doi: 10.1117/1.NPh.10.2.023513.

[7] E. M. Frijia *et al.*, "Functional imaging of the developing brain with wearable high-density diffuse optical tomography: A new benchmark for infant neuroimaging outside the scanner environment," *Neuroimage*, vol. 225, p. 117490, Jan. 2021, doi: 10.1016/j.neuroimage.2020.117490.

[8] L. Katus *et al.*, "Longitudinal fNIRS and EEG metrics of habituation and novelty detection are correlated in 1–18-month-old infants," *Neuroimage*, vol. 274, p. 120153, Jul. 2023, doi: 10.1016/j.neuroimage.2023.120153.

[9] L. Pirazzoli *et al.*, "Association of psychosocial adversity and social information processing in children raised in a low-resource setting: an fNIRS study," *Dev Cogn Neurosci*, vol. 56, p. 101125, Aug. 2022, doi: 10.1016/j.dcn.2022.101125.

[10] S. Brigadoi *et al.*, "Motion artifacts in functional near-infrared spectroscopy: A comparison of motion correction techniques applied to real cognitive data," *Neuroimage*, vol. 85, pp. 181–191, Jan. 2014, doi: 10.1016/j.neuroimage.2013.04.082.

[11] J. W. Barker, A. L. Rosso, P. J. Sparto, and T. J. Huppert, "Correction of motion artifacts and serial correlations for real-time functional near-infrared spectroscopy," *Neurophotonics*, vol. 3, no. 3, p. 031410, May 2016, doi: 10.1117/1.NPh.3.3.031410.

[12] J. Zhao, J. Qiao, X. Ding, and X. Liang, "fNIRS Signal Motion Correction Algorithm Based on Mathematical Morphology and Median Filter," *Acta Optica Sinica*, vol. 40, no. 22, p. 2230002, 2020, doi: 10.3788/AOS202040.2230002.

[13] Y. Gao *et al.*, "Deep learning-based motion artifact removal in functional near-infrared spectroscopy," *Neurophotonics*, vol. 9, no. 04, Apr. 2022, doi: 10.1117/1.NPh.9.4.041406.

[14] F. Scholkmann, S. Spichtig, T. Muehlemann, and M. Wolf, "How to detect and reduce movement artifacts in near-infrared imaging using moving standard deviation and spline interpolation," *Physiol Meas*, vol. 31, no. 5, pp. 649–662, May 2010, doi: 10.1088/0967-3334/31/5/004.

[15] J. Selb *et al.*, "Effect of motion artifacts and their correction on near-infrared spectroscopy oscillation data: a study in healthy subjects and stroke patients," *J Biomed Opt*, vol. 20, no. 5, p. 056011, May 2015, doi: 10.1117/1.JBO.20.5.056011.

[16] B. P. Welford, "Note on a Method for Calculating Corrected Sums of Squares and Products," *Technometrics*, vol. 4, no. 3, pp. 419–420, Aug. 1962, doi: 10.1080/00401706.1962.10490022.

[17] "ALINX AXU3EG or AXU3EGB: Ethernet FPGA development board." Accessed: Oct. 21, 2023. [Online]. Available: https://www.xilinx.com/products/boards-and-kits/1-1cm64x4.html

[18] T. J. Huppert, S. G. Diamond, M. A. Franceschini, and D. A. Boas, "HomER: a review of time-series analysis methods for near-infrared spectroscopy of the brain," *Appl Opt*, vol. 48, no. 10, p. D280, Apr. 2009, doi: 10.1364/AO.48.00D280.